O(6)-symmetry breaking in the γ-soft nucleus ^{126}Xe and its evolution in the light stable xenon isotopes

L. Coquard,[1] G. Rainovski,[1,2] N. Pietralla,[1] T. Ahn,[1,3] L. Bettermann,[4] M. P. Carpenter,[5] R. V. F. Janssens,[5] J. Leske,[1] C. J. Lister,[5] O. Möller,[1] T. Möller,[1] W. Rother,[4] V. Werner,[3] and S. Zhu[5]

[1]*Institut für Kernphysik, Technische Universität Darmstadt, D-64289 Darmstadt, Germany*
[2]*Faculty of Physics, St. Kliment Ohridski University of Sofia, BG-1164 Sofia, Bulgaria*
[3]*Wright Nuclear Structure Laboratory, Yale University, New Haven, Connecticut 06520, USA*
[4]*Institut für Kernphysik, Universität Köln, Zülpicher Strasse 77, D-50937 Köln, Germany*
[5]*Physics Division, Argonne National Laboratory, Argonne, Illinois 60439, USA*

(Received 19 November 2010; published 25 April 2011)

Low-lying collective states in ^{126}Xe have been investigated via the ^{12}C(^{126}Xe,^{126}Xe*) projectile Coulomb excitation reaction at 399 MeV. The γ decays were detected with the Gammasphere array. Coulomb excitation cross sections relative to the 2_1^+ state were obtained. Twenty-two absolute $E2$ transition strengths have been deduced. An *sd*– interacting boson model (IBM-1) fit agrees well with the new experimental data. This makes a quantitative test of O(6)-symmetry breaking in ^{126}Xe possible. The measured absolute $B(E2)$ values indicate a preservation of O(5) symmetry, while the O(6) symmetry is broken. The evolution of O(6)-symmetry breaking and of O(5)-symmetry conservation in the ^{124,126,128}Xe isotopic chain is discussed.

DOI: 10.1103/PhysRevC.83.044318 PACS number(s): 21.10.Re, 23.20.Js, 25.70.De, 27.60.+j

I. INTRODUCTION

Atomic nuclei are many-body fermionic quantum systems whose dynamics is governed by the strong nuclear interaction. The strongly coupled many-body nature leads to collective motion of nucleons governed by the symmetries of the residual interactions between them. Those symmetries manifest themselves as regular sequences of excited levels and through certain simple selection rules for their electromagnetic decays. The question of how such well-pronounced, simple behavior arises from the complex motion of many strongly interacting fermions and of how this behavior evolves as a function of nucleon number has been and is still one of the central issues in nuclear structure research. There are two extreme approaches to this question. One is to utilize the semiclassical concept of nuclear shapes at the expense of sacrificing the link to the contribution of individual nucleons. The second approach is to perform microscopic calculations. The solution of this problem in the full configuration space remains a considerable computational challenge, which, in practice, can be solved for heavy nuclei only after considerable truncations. One intermediate approach for describing the low-lying quadrupole collective modes in even-even nuclei was suggested in terms of the interacting boson model (IBM-1) [1,2]. The IBM-1 model considers the valence nucleons coupled into boson pairs with spins $J = 0$ (s boson) and $J = 2$ (d boson) only.

The IBM-1 Hamiltonian possesses inherent U(6) symmetry, which can be used as a powerful algebraic tool for classifying the nature of low-lying collective states of even-even nuclei into three symmetry classes: U(5) [3], SU(3) [4], and O(6) [5]. The presence of a symmetry is related to the conservation of certain quantum numbers. At these dynamical symmetries, the IBM Hamiltonian is analytically solvable [1,2], and the solutions are directly related to analytically solvable cases of the geometrical Bohr Hamiltonian [6], the harmonic vibrator, the quadrupole-deformed axial rotor, and the γ-unstable rotor [7], respectively. The existence of any of the dynamical symmetries is experimentally established by observing the specific energy-level patterns and decays that follow the associated selection rules. Exact realizations of the dynamical symmetries are not manifested in nature, but finding nuclei that behave closely to them is an important task because such systems serve as benchmarks for the evolution of nuclear collectivity. Moreover, such benchmark nuclei also show to what extent the bosonic approximation holds for the fermionic nuclear many-body problem.

The experimental observation of O(6) symmetry in nuclei is scarce. The best established case is ^{196}Pt [8,9]. Also, the Xe-Ba-Ce nuclei in the $A \approx 130$ region are considered as exhibiting O(6)-like behavior [10]. The stable even-even xenon isotopes, $^{124-132}$Xe, were considered to be part of this extensive O(6)-like region. Indeed, the low-spin structures of ^{128}Xe [11], ^{126}Xe [12], and ^{124}Xe [13] manifest O(6)-like arrangements of energy levels [10] and $E2$ branching ratios reflecting the selection rules of the O(5) symmetry, where O(5) is a subgroup of O(6). However, this interpretation was challenged very recently in the case of ^{124}Xe [14]. It has now been shown quantitatively that the O(6) symmetry is severely broken, while the O(5) symmetry holds well. This surprising result for ^{124}Xe [14] naturally leads one to question to what extent the O(6) symmetry is broken or preserved in the neighboring xenon isotopes. Such an unambiguous and quantitative study of symmetry breaking and preservation requires a complete set of absolute $E2$ transition strengths, especially the ones associated with transitions between states from different O(6) quantum numbers σ and O(5) quantum numbers τ. These absolute $E2$ transition strengths test the validity of the selection rules directly; in the cases of O(6) and O(5) symmetries, $E2$ transitions are allowed between states with $\Delta\sigma = 0$ and $\Delta\tau = \pm 1$. This experimental information is rarely available, but it has been shown [14–16] that projectile

Coulomb excitation can serve as a powerful tool to obtain it. The purpose of the present study is to investigate the ^{126}Xe low-spin states with projectile Coulomb excitation. The information obtained on the absolute $E2$ transition strengths allows us to quantify the degree of O(6)-symmetry breaking or preservation in this nucleus, following the method outlined in Ref. [14]. The same analysis is carried out for ^{128}Xe using the results from Ref. [15]. Altogether, information is provided on the evolution of O(6)-symmetry breaking and preservation in the chain of xenon isotopes when the neutron number approaches the $N = 82$ shell closure.

II. EXPERIMENT

The experiment was performed at Argonne National Laboratory. The superconducting ATLAS linear accelerator provided a beam of ^{126}Xe ions with an energy of 399 MeV, which corresponds to ∼80% of the Coulomb barrier for reactions on a ^{12}C target [17]. The beam intensity was ∼1 pnA. The beam was pulsed (12 MHz) and impinged on a natural ^{12}C target of 1-mg/cm^2 thickness. The emitted γ rays were detected by the Gammasphere array, which consisted of 98 high-purity Compton-suppressed germanium detectors arranged in 16 rings [18,19]. The event trigger was defined by detection of a single γ ray, but higher-multiplicity events were recorded as well. The average trigger readout rate was 15 000 events/s (readout dead time was ∼30%). This count rate compares with a "beam-off" rate of 600 events/s. The total number of recorded events was 1.3×10^9 for a running time of ∼29 h and approximately 1.8×10^7 events of γ-ray fold higher than 1 were sorted into a $\gamma\gamma$-coincidence matrix. Doppler correction (recoiling velocity $\beta = 6.4(2)\%$) and time-random background subtraction was applied. As the beam energy was relatively low, the dominant beam-off count rate came from natural sources. This background was identified and subtracted by selecting events occurring between the beam bursts, scaled to eliminate the 1461-keV decay from ^{40}K. The singles spectrum is displayed in Fig. 1.

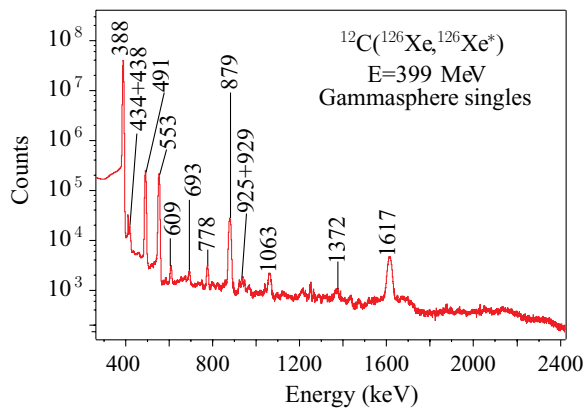

FIG. 1. (Color online) Background-subtracted and Doppler-corrected single γ-ray spectrum for the sum over all Ge detectors following ^{126}Xe Coulomb excitation on a ^{12}C target.

III. DATA ANALYSIS

All the γ transitions observed have been placed in the ^{126}Xe level scheme, and their corresponding intensities are listed in Table I. They were reported previously in Refs. [12,20,21], except for the 1373-keV line originating from the decay of the 3^-_2 state at 2315 keV to the 4^+_1 level at 942 keV. The γ-ray intensities have been normalized to the $2^+_1 \rightarrow 0^+_1$ ground-state transition, which dominates the spectrum by three orders of magnitude. The population yields of each state have been deduced from γ singles and $\gamma\gamma$-coincidence data. The contribution from the electron conversion decays was small in comparison to the systematic errors (<1.5%, [22]) and has been neglected. The contributions of known transitions that were not observed (e.g., due to their too low energy or the presence of contaminants) have been determined from previously published branching ratios [23].

The observed relative yields measure the Coulomb excitation (CE) cross sections relative to the 2^+_1 state. The multiple-Coulex code CLX, based on the Winther–De Boer theory [24], has been used to determine the set of matrix elements that reproduce the observed relative cross sections. The previously known $B(E2; 2^+_1 \rightarrow 0^+_1) = 0.152(5)\, e^2b^2$ value from Ref. [23] sets the absolute scale. The energy loss of the beam inside the target (∼40 MeV) was taken into account. The unknown quadrupole moments of excited states were allowed to vary between the extreme rotational limits ($Q = \pm 2.78$ e b), adding uncertainties of 5%, on average, to the transitional matrix elements. The input matrix elements in CLX were also constrained by the known branching and multipole mixing ratios. The choice of sign of the matrix elements is not always unique in a fit to multistep Coulomb excitation processes. However, constraints come from the requirement that the relative phases must be "quantum mechanically coherent." The signs of the $E2$ matrix elements were chosen to be in agreement with those predicted by the IBM-1 calculation described below and are also listed in Table I for clarity (σ). In addition to the statistical uncertainties, the final results in Table I include uncertainties from all quantities varied or constraining the variations in the procedure described above, e.g., branching ratios, multipole ratios, and unknown quadrupole moments.

IV. RESULTS

The resulting $B(E2)$ transition strengths are given in Table I. The present analysis resulted in 22 absolute values and 7 upper limits for the $B(E2)$ strengths. Due to their small values, the $B(M1)$ transitions strengths have been omitted in Table I, except for the relevant upper limit obtained for the transition of the 2^+ state at 2455 keV to the 2^+_1 level.

(i) 4^+_1 level at 942 keV. The unobserved $4^+_1 \rightarrow 2^+_2$ transition at 62 keV does not play a significant role for the population of the 4^+_1 state at 942 keV. Another issue with the population of the 4^+_1 state is the contribution of a one-step $E4$ excitation. Since it was impossible to quantify or estimate this $B(E4)$ transition strength, the $B(E2; 4^+_1 \rightarrow 2^+_1)$ value in Table I assumes no $E4$ transition from the ground state.

TABLE I. Measured properties of the levels and γ-ray transitions in ^{126}Xe. The absolute $E2$ strengths are compared to sd–IBM-1 calculations.

E_{level} (keV)	J^π	E_γ (keV)	I_γ	J^π_{final}	δ[a]	σ	Transition strength[b]		τ
							Exp.	IBM-1	(ps)
388	2^+_1	388	10^6	0^+_1		+	41.0(13)[b]	41.0	58.8(19)[c]
879	2^+_2	491	7836(58)	2^+_1	$+9.1^{+43}_{-2}$	−	43.2(26)	48.9	13.5(17)
		879	2134(17)	0^+_1		+	0.63(7)	0.65	
942	4^+_1	63[d]		2^+_2		−		0.01	5.9(6)
		553	7655(56)	2^+_1		+	71.0(67)	58.9	
1314	0^+_2	434[e]	11.1(18)	2^+_2		+	64(9)	58.0	4.36(54)
		925[e]	45.4(21)	2^+_1		−	5.9(9)	5.51	
1317	3^+_1	376[f]	1.43(28)	4^+_1		−	$\leqslant$22.1(13)[g]	15.9	11.8(12)
		438[e]	7.7(15)	2^+_2	$+8^{+3}_{-2}$	+	55.7(63)	45.0	
		929[e]	7.3(15)	2^+_1	$+1.6^{+3}_{-7}$	−	0.90(23)	0.91	
1488	4^+_2	546[e]	35.6(6)	4^+_1	$+3.0^{+10}_{-9}$	+	28.3(38)	25.8	4.2(3)
		609	70.7(9)	2^+_2		−	36.1(42)	33.2	
		1100[e]	14.9(3)	2^+_1		−	0.40(8)	0.14	
1635	6^+_1	693	54.7(18)	4^+_1		+	84(11)	64.8	1.64(21)
1678	2^+_3	361[e,h]	5.1(20)	3^+_1		−	$\leqslant$20.6(44)[g]	28.3	9.1(9)
		364[e,h]	9.8(21)	0^+_2		+	38.3(91)	23.1	
		736[f]	8.54(53)	4^+_1		−	0.96(4)	1.36	
		799[h]	24.1(14)	2^+_2		+	$\leqslant$1.86(41)[g]	0.23	
		1290[f]	14.7(9)	2^+_1		−	$\leqslant$0.10(2)[g]	0.002	
		1678[f]	33.8(21)	0^+_1		−	0.063(14)	0.02	
1760	0^+_3	881[h]	7.8(16)	2^+_2		−	13.4(41)	4.75	0.36(8)
		1372[h]	58.6(22)	2^+_1		−	10.9(25)	11.1	
2005	3^-_1	1063	166(4)	4^+_1					
		1126[h]	29.1(18)	2^+_2					
		1617	885(11)	2^+_1					
		2005		0^+_1		+	B(E3) = 0.090(15)[i]		
2086	2^+_5	326[j]		0^+_3		+	11÷48	23.4	$\leqslant$2.1(5)[k]
		1144[f]	10.4(11)	4^+_1		−	1.63(16)	4.9	
		1207[h]	18.2(15)	2^+_2	$+0.9^{+5}_{-3}$	+	0.99(61)	3.0	
		2086[f]	4.99(58)	0^+_1		−	0.04(1)	0.07	
2301	$5^{(-)}$	1359[h]	15.6(12)	4^+_1					
2315	$3^{(-)}$	1373[h]	14.2(11)	4^+_1					
		1435[h]	31.1(18)	2^+_2					
2414	$5^{(-)}$	1472[h]	13.7(11)	4^+_1					
2455	2^+	1138[f]	0.81(10)	3^+_1		+	$\leqslant$1.96(60)[g]	0.0002	0.20(4)
		1514[f]	1.36(15)	4^+_1		−	0.79(25)	0.0015	
		1576[f]	3.66(39)	2^+_2		−	$\leqslant$1.76(52)[g]	0.0009	
		2067[h]	14.8(15)	2^+_1		−	$\leqslant$1.82(54)[g]	0	
				2^+_1			$B(M1) \leqslant 0.020(6)$[g]	0	
		2455[f]	2.69(30)	0^+_1		+	0.14(4)	0	

[a]The multipole mixing ratios are taken from Ref. [23].

[b]$B(E2)$ values are given in W.u. (1 W.u.$(E2) = 0.003752\ e^2\text{b}^2$), $B(M1)$ are given in μ_N^2, and the $B(E3; 0^+_1 \rightarrow 3^-_1) \uparrow$ value is given in $e^2\text{b}^3$.

[c]Adopted value taken from Ref. [25].

[d]This transition is not observed. Contrary to Ref. [14], this transition does not play a relevant role for the population of the 4^+_1 state.

[e]These transitions are doublets, the individual intensities have been separated using the known branching ratios taken from Ref. [23].

[f]Determined through the branching ratio from Ref. [23].

[g]Upper limits since the mixing ratio was unknown; $B(E2)$ and $B(M1)$ upper limits are given under the assumption of either pure $E2$ or pure $M1$ transitions, respectively.

[h]This transition was observed only in coincidence spectra.

[i]In Ref. [26], a $B(E3) \uparrow = 0.085(13)\ e^2\text{b}^3$ value is reported.

[j]This transition is not observed directly, but it is included in the calculations for the Coulomb cross sections for a best match with the data.

[k]Upper limit since only a lower limit of the total width (Γ_{tot}) of the state has been measured.

(ii) 0_2^+ level at 1314 keV and 3_1^+ level at 1317 keV. The 0_2^+ state at 1314 keV decays through the 434-keV γ ray to the 2_2^+ level and through the 925-keV transition to the 2_1^+ level. These lines are doublets with the two γ rays coming from the 3_1^+ level at 1317 keV. This 3_1^+ state decays also to the 2_2^+ level with $E_\gamma = 438$ keV and to the 2_1^+ level with $E_\gamma = 925$ keV. The energy resolution achieved here did not permit us to resolve these two doublets. Therefore, the intensities of each doublet were fitted and the previously known branching ratios [23] were used to obtain the individual respective intensities.

(iii) 4_2^+ level at 1488 keV. Similarly, the 546-keV γ ray from the 4_2^+ level at 1488 keV to the 4_1^+ level is a doublet with strong 553-keV transition. The individual intensity of the 546-keV γ ray has been deduced from the known branching ratio [23] and the measured intensity of the $4_2^+ \rightarrow 2_2^+$, 609-keV transition. Again, no $E4$ transition from the ground state was considered in the Coulomb excitation process.

(iv) 2_3^+ level at 1678 keV. The mixing ratio for the $2_3^+ \rightarrow 2_1^+$ transition is unknown. Due to low statistics, the present data did not enable an angular distribution measurement. In Table I, the mixed transitions coming from this state have been calculated by assuming pure $E2$ character, hence the resulting upper limits. However, assuming that the $2_3^+ \rightarrow 2_1^+$ transition is of pure $M1$ character results in a $B(M1; 2_3^+ \rightarrow 2_1^+) \leqslant 4.35(87) \times 10^{-4}\ \mu_N^2$ value. This small strength rules out the possibility that this state could be a sizable fragment of the one-phonon $2_{1,\mathrm{ms}}^+$ mixed-symmetry state [27].

(v) 2_5^+ level at 2086 keV. This state does not decay to the 2_1^+ level, which rules out the possibility that it could have mixed-symmetry character. The $2_5^+ \rightarrow 0_3^+$ transition is not observed either. However, the existence of this transition cannot be ruled out due to the large energy suppression factor for its intensity ($E_\gamma = 326$ keV). This transition was included in the CLX calculations, showing that the yields of the 2_5^+ and the 0_3^+ states are barely influenced by the size of the $\langle 0_3^+ || E2 || 2_5^+ \rangle$ matrix element. A $B(E2; 2_5^+ \rightarrow 0_3^+)$ value below $\sim$50 W.u. will influence the yields of the 2_5^+ and 0_3^+ states within their experimental error bars only.

(vi) 2^+ level at 2455 keV. Since the mixing ratio for this $2^+ \rightarrow 2_1^+$ transition is unknown [23], a pure $E2$ transition was assumed, leading to an upper value $B(E2; 2^+ \rightarrow 2_1^+) \leqslant 1.82(54)$ W.u. Assuming pure $M1$ multipolarity results in $B(M1; 2^+ \rightarrow 2_1^+) \leqslant 0.020(6)\ \mu_N^2$. This small value rules out a mixed-symmetry character for this state.

The experimental low-lying energy level scheme of ^{126}Xe is displayed in Fig. 2(a). Figure 2(b) provides the corresponding energy-level spectrum stemming from the *sd*–IBM-1 fit described in the next section.

V. DISCUSSION

In order to quantify the degree of symmetry breaking in ^{126}Xe, the procedure outlined in Ref. [14] was followed. The *sd*–IBM-1 Hamiltonian was used,

$$H = \epsilon n_d + \left(\lambda + \frac{2}{5}\beta\right) L \cdot L + \kappa Q^\chi \cdot Q^\chi + 4\beta T^{(3)} \cdot T^{(3)}, \tag{1}$$

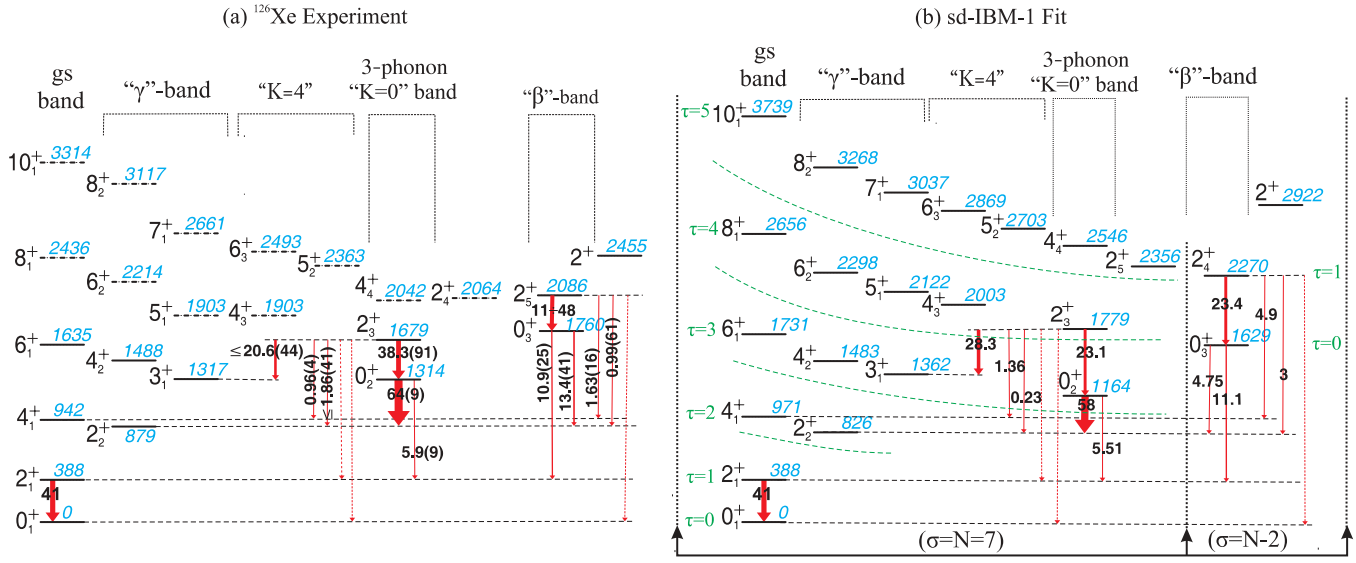

FIG. 2. (Color online) (a) Low-energy, positive-parity levels of ^{126}Xe. The levels observed in the present experiment are represented by solid lines. Dashed lines indicate energy levels known from the literature [23]. (b) The *sd*–IBM-1 calculation for ^{126}Xe (see text). The eigenstates are arranged in (τ, σ) multiplets according to the O(6) dynamical symmetry. The arrows represent the $E2$ transitions for off-yrast, quasi-$K = 0$ levels of particular interest. The thickness of the arrows and the numbers associated with them correspond to the absolute $B(E2)$ values in W.u. The dashed arrows are transitions with $B(E2) \leqslant 0.1$ W.u.

similar to recent studies [13,14] with the fitted parameters $\epsilon_0 = 0.712$ MeV, $\beta_0 = -23.0$ keV, $\lambda_0 = 13.5$ keV, $\chi_0 = 0.180$, $\kappa_0 = -41.9$ keV, and $e_B = 0.12246\ e^2\text{b}^2$. The positive sign of parameter χ_0 is chosen in order to reproduce consistently the Coulomb excitation yields of states populated by only multistep processes. For a more detailed discussion on the procedure for obtaining the Hamiltonian's parameters, the reader is referred to Refs. [13,28]. The results from this numerical IBM calculation (done with the code PHINT [29]) are presented in the rightmost column of Table I and in Fig. 2(b). All calculated absolute $E2$ transition strengths must be considered as predictions, except for the $2_1^+ \rightarrow 0_1^+$ transition. The agreement between the calculated and the experimental $B(E2)$ values is good for all observed $E2$ transitions. The agreement for the energy levels is also satisfactory (Fig. 2). It is worth emphasizing that the IBM parametrization obtained here is capable of describing the present comprehensive data set in a consistent way. This provides confidence that the calculated wave functions represent the nuclear quantum states in the framework of the IBM correctly. The structure including the ground-state band, the quasi-γ band, the quasi-$K = 4$ band, and the quasi-$K = 0$ band residing on top of the 0_2^+ state reflects the expected pattern of a $\sigma = N$ structure in the O(6) symmetry. Correspondingly, the structure denoted by the quasi-β band could be expected to represent a realization of a structure with the O(6) quantum number $\sigma = N - 2$. Surprisingly, this is not the case. For a quantitative analysis of the presence of the O(6) and O(5) symmetries, the wave functions for the first few 0^+ and 2^+ IBM states have been projected onto the O(6) basis $\{|J^\pi\rangle^{(\sigma,\tau)}\}$, and the results are presented in Fig. 3.

From Fig. 3, it is obvious that neither τ nor σ are perfect quantum numbers. However, τ quantum numbers appear to be quite well preserved, which indicates that O(5) is the relevant symmetry. The components with a "correct" τ quantum number exhaust about 90% or more of the total wave functions. The best example is the ground state where more than 99% of the wave function contains the right $\tau = 0$ number. The small admixtures with different τ values are such that the deviations from the O(5) selection rules can easily be explained. For example, the wave function of the 0_2^+ state, the bandhead of the three phonon $K = 0$ structure [Fig. 2(b)], contains a small component with $(\sigma = 7, \tau = 0)$, which has an amplitude of about 1.4% (see Fig. 3). This component makes an allowed $(\Delta\sigma = 0, \Delta\tau = -1)$ $E2$ transition to the main component of the 2_1^+ state possible. This 2_1^+ level, in turn, has the correct $(\sigma = 7, \tau = 1)$ quantum numbers and an amplitude of about 70%. At the same time, the main component of the 0_2^+ state with $(\sigma = 7, \tau = 3)$ quantum numbers can proceed through an allowed transition to the component of the 2_1^+ state with $(\sigma = 7, \tau = 2)$. Analogously, the components with $(\sigma = 5, \tau = 0)$ and $(\sigma = 3, \tau = 0)$ of the 0_2^+ level can make allowed transitions to the components with $(\sigma = 5, \tau = 1)$ and $(\sigma = 3, \tau = 1)$ of the 2_1^+ state (see Fig. 3). All these $\Delta\tau$ allowed contributions can add up and result in the mildly collective $0_2^+ \rightarrow 2_1^+$ transition observed experimentally [see Fig. 2(a)]. In the same way, the small components with "incorrect" τ and σ in the wave functions of the 0_3^+ and the 2_1^+ IBM states are the main reasons for the existence of the otherwise forbidden $0^+_{\text{"}\beta\text{"}} \rightarrow 2_1^+$ transition, while main contributions to the collective $E2$ transition between the 2_4^+ and the 0_3^+ states come mostly from components with $\Delta\tau = \pm 1$.

The σ quantum numbers do, however, appear to have little or no validity (again, see Fig. 3). Even the ground state contains only 63.1% of $\sigma = N = 7$ value. For the states that were thought to belong to the $\sigma = N - 2 = 5$ representation, the 0_3^+ and the 2_4^+ levels, the σ quantum number is completely diluted. In fact, the components with $\sigma = 5$ account only for 20.2% and 42.3% of the total wave functions of these IBM states (Fig. 3).

In an attempt to quantify the amount of symmetry breaking, the fluctuations Δq in the quantum number of states are considered, where $\Delta q = \sqrt{\langle q^2\rangle - \langle q\rangle^2}$, with q representing the quantum number related to the symmetry under consideration. For further details concerning the fluctuation analysis, the reader is referred to Ref. [14]. For an exact symmetry, $\Delta q = 0$ for all states. All the other cases represent a situation with broken symmetry. A perturbed and dissolved symmetry is defined by the classification value $\Delta q_{\text{class}} \equiv \delta q_{\text{min}}/(2\sqrt{2ln2})$,

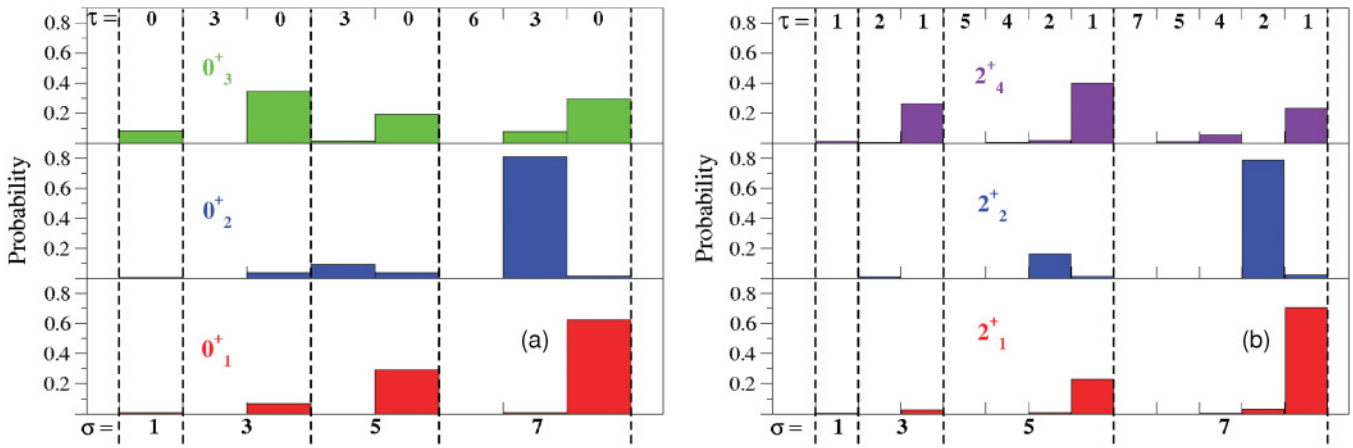

FIG. 3. (Color online) Squared amplitudes of the components with different (σ, τ) values in (a) the $0^+_{1,2,3}$ and (b) the $2^+_{1,2,4}$ sd–IBM-1 wave functions.

where $\delta q_{\min}$ is the minimum step the quantum number q can change (e.g., $\delta\sigma_{\min} = 2$). The symmetry is then considered to be *perturbed, but dominant*, if the fluctuations in the quantum number are $\Delta q \leqslant \Delta q_{\text{class}}$. For $\Delta q > \Delta q_{\text{class}}$ the symmetry related to this quantum number is viewed as *dissolved*. The classification values obtained for the O(6) symmetry and the O(5) symmetry are $\Delta\sigma_{\text{class}} = 0.849$ and $\Delta\tau_{\text{class}} = 0.425$, respectively.

In Ref. [14], it was proposed that the degree of symmetry breaking or preservation is quantified by the fluctuation in the respective quantum number [σ in the case of O(6) and τ in the case of O(5)] for states whose decay are sensitive to a particular selection rule. For testing the O(6) symmetry, such a state is the bandhead of the quasi-β band, while the decay of the bandhead of the quasi-γ band is sensitive to the O(5) selection rules. Indeed, the $2^+_{\gamma''} \to 0^+_1$ transition is σ allowed and τ forbidden, while the $0^+_{\beta''} \to 2^+_1$ transition is σ forbidden and τ allowed.

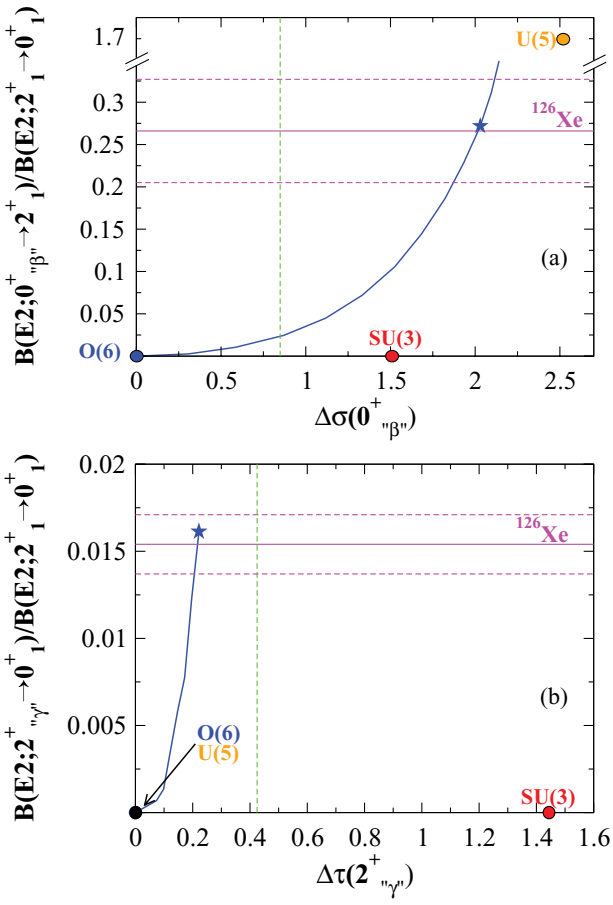

FIG. 4. (Color online) Evolution of the (a) $B(E2; 2^+_{\beta''} \to 2^+_1)/B(2^+_1 \to 0^+_1)$ and the (b) $B(E2; 2^+_{\gamma''} \to 0^+_1)/B(2^+_1 \to 0^+_1)$ ratios as functions of $\Delta\sigma$ and $\Delta\tau$ (solid curves) on the linear trajectory from the exact O(6) symmetry to the point defined by the IBM-1 parameters described in this work (stars). The vertical dashed lines represent the classification values of $\Delta\sigma$ and $\Delta\tau$ beyond which the respective symmetry is dissolved. The circles represent the values of the respective ratios and the fluctuations at the U(5) and SU(3) dynamical symmetries of the IBM. The horizontal lines represent the experimental values in ^{126}Xe.

Therefore, the quantum number fluctuations in the $0^+_{\beta''}$ and the $2^+_{\gamma''}$ states are considered to be measures for the symmetry breaking and preservation of O(6) and O(5) symmetries for the entire nucleus, respectively. To trace the evolution of these observables through the parameter space of the IBM-1 from the exact O(6) symmetry to the point defined by the model parameters of Eq. (1), the following parametrization was used: $\beta(a) = \beta_{\text{O(6)}} + a(\beta_W - \beta_{\text{O(6)}})$, $\epsilon(a) = \epsilon_0 a$, and $\chi(a) = \chi_0 a$ [14]. When $a = 1$, H is the Hamiltonian found to best describe ^{126}Xe. For $a = 0$, the IBM Hamiltonian corresponds to the exact O(6) symmetry. The parameter $\beta_{\text{O(6)}}$ was also arbitrarily fixed with $\beta_{\text{O(6)}} = -0.455$ keV in order to obtain the head of the $\sigma = N - 2$ structure as the third 0^+ state in the exact O(6) symmetry ($a = 0$). The evolutions of the two observables sensitive to the O(6) and O(5) symmetries $B(E2; 0^+_{\beta''} \to 2^+_1)/B(E2; 2^+_1 \to 0^+_1)$ and $B(E2; 2^+_{\gamma''} \to 0^+_1)/B(E2; 2^+_1 \to 0^+_1)$ with $\Delta\sigma$ and $\Delta\tau$ are plotted in Figs. 4(a) and 4(b), respectively.

A comparison between the evolution of the $B(E2; 0^+_{\beta''} \to 2^+_1)/B(E2; 2^+_1 \to 0^+_1)$ ratio and the experimental value measured for ^{126}Xe [Fig. 4(a)] provides the value $\Delta\sigma_{\text{exp}}(0^+_3; ^{126}\text{Xe}) = 2.03^{+0.08}_{-0.16}$, which lies well beyond the classification value of 0.849 and is comparable to the fluctuations observed in the σ quantum number for the other dynamical symmetries, U(5) and SU(3). The latter are also presented in Fig. 4(a). The large value of $\Delta\sigma_{\text{exp}}$ obtained for the $0^+_{\beta''}$ state of ^{126}Xe implies that the O(6) symmetry is severely broken, in fact, to an extent comparable to the degree of breaking of this symmetry in other dynamical limits. For the 0^+_3 state of ^{126}Xe, which was a candidate for the lowest $\sigma = N - 2$ state, the O(6) symmetry is actually completely dissolved. In contrast, Fig. 4(b) provides $\Delta\tau_{\text{exp}}(2^+_2; ^{126}\text{Xe}) = 0.221(14)$, a value lying well below the classification value of 0.425, which indicates that the O(5) symmetry is preserved.

The calculations of the σ and τ fluctuations can also be extended to ^{128}Xe by using the results of Ref. [15]. The fitted parameters of the Hamiltonian of Eq. (1) for ^{124,126,128}Xe are summarized in Table II. In the case of ^{128}Xe, these parameters do not reproduce well the positions and the decays of the two first excited 0^+ states. Therefore, the fluctuations have been calculated by using the IBM parameters reproducing best the experimental $B(E2; 0^+_{\beta''} \to 2^+_1)/B(E2; 2^+_1 \to 0^+_1)$ ratio (i.e., for $a = 0.7$). In this case, $\Delta\sigma_{\text{exp}}(0^+_3; ^{128}\text{Xe}) = 1.55^{+0.12}_{-0.08}$ and $\Delta\tau_{\text{exp}}(2^+_2; ^{128}\text{Xe}) = 0.19^{+0.03}_{-0.01}$. If we would have calculated the fluctuations at the point corresponding to the parameters for ^{128}Xe in Table II, we would have found slightly larger values of $\Delta\sigma_{\text{exp}}(0^+_3; ^{128}\text{Xe}) = 1.81$ and $\Delta\tau_{\text{exp}}(2^+_2; ^{128}\text{Xe}) = 0.20$. We

TABLE II. Parameters used in the *sd*–IBM-1 Hamiltonian for ^{128,126}Xe and comparison with the parameters found in Ref. [13] for ^{124}Xe.

	ϵ_0/κ_0	χ_0	β_0/κ_0	λ_0/κ_0	κ_0 (keV)	e_B (e b)
^{128}Xe	−16.8	+0.173	0.76	−0.245	−53.0	0.115
^{126}Xe	−17.0	+0.180	0.55	−0.322	−41.9	0.122
^{124}Xe	−20.9	−0.257	0.563	−0.284	−34.91	0.142

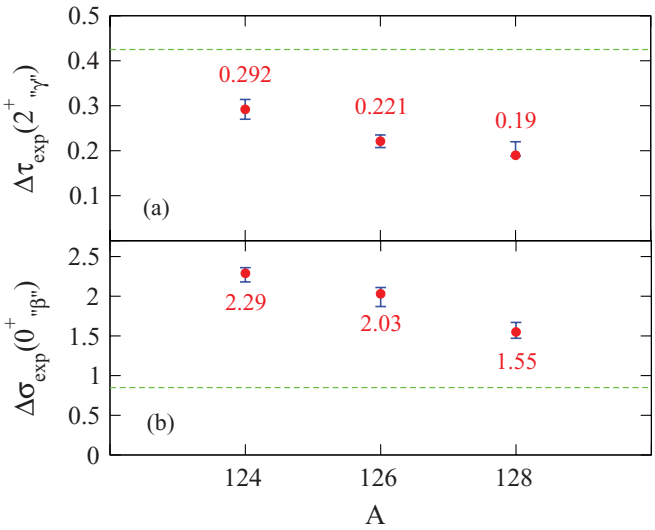

FIG. 5. (Color online) Evolution of the (a) τ and (b) σ fluctuations characterizing the degree of O(5)-symmetry preservation and O(6)-symmetry breaking in ^{124,126,128}Xe. The horizontal dashed lines represent the classification values above which the symmetry is broken and under which the symmetry is preserved.

want to stress that in both cases the fluctuations in σ and τ quantum numbers in ^{128}Xe are smaller than the ones for ^{126}Xe.

The τ and σ fluctuations for the three isotopes ^{124,126,128}Xe are plotted in Figs. 5(a) and 5(b), respectively. In these three Xe isotopes, it is observed that the O(6) symmetry is broken [Fig. 5(b)], with the breaking being more pronounced in ^{124}Xe and gradually decreasing with increasing number of nucleons. On the contrary, the τ fluctuations lie always below the classification value [Fig. 5(a)], which indicates that the O(5) symmetry is only slightly perturbed in ^{124,126,128}Xe. It is worth stressing that such an analysis is made possible only by the comprehensive set of absolute values of $E2$ transition rates available from projectile Coulomb excitation measurements on a light target combined with an sd–IBM-1 fit. The equivalent $B(E2)$ decay rates from the 0_3^+ level are, at present, unknown in ^{130}Xe and ^{132}Xe. Thus, the degree of O(6)-symmetry breaking in these two isotopes cannot be quantified in the same way. However, these nuclei already lie beyond the region of the O(6) symmetry. Indeed, in Refs. [15,30], ^{130}Xe was proposed as the best candidate among stable even-even Xe isotopes for the E(5) symmetry, and ^{132}Xe, with only two pairs of valence neutrons away from the closed shell $N = 82$, is already close to the U(5) symmetry, a feature that applies even more to ^{134}Xe.

To conclude, it has been shown that none of the stable even-even Xe isotopes should be considered as possessing the O(6) symmetry of the IBM. The exclusion of the stable xenon isotopes from the set of nuclei with dominant O(6) symmetry raises questions about the extent to which any nucleus from the $A = 130$ mass region can achieve O(6) symmetry.

VI. SUMMARY

^{126}Xe has been studied using projectile Coulomb excitation. In total, 22 absolute $E2$ transition strengths between low-spin states have been determined. The experimentally observed level energies, branching ratios, and the absolute transition strengths are reproduced well by a general sd–IBM-1 calculation outside any dynamical symmetry. Symmetry breaking (or preservation) was investigated by relating the fluctuations in the quantum numbers directly to the experimental observables, as suggested in Ref. [14]. In ^{126}Xe, the O(6) symmetry was found to be completely dissolved, while the O(5) symmetry is only slightly perturbed. By using the same approach in ^{128}Xe, a similar result was obtained. The evolution of the O(6)- and O(5)-symmetry breaking and preservation as a function of neutron number for the light stable xenon isotopes indicates a tendency of approaching the O(6) limit, but without ever reaching it in the xenon isotopes. As a result, a similar detailed investigation of the Ce, Ba, and Pt isotopes, which have been previously associated with the O(6) symmetry, appears to be warranted.

ACKNOWLEDGMENTS

We would like to thank the staff at ANL for their support during the experiments and A. Poves, F. Iachello, J. Jolos, J. Jolie, A. Dewald, and P. von Brentano for discussions. G.R. was supported by the Alexander von Humboldt Foundation. This work was partially supported by the US Department of Energy, Office of Nuclear Physics, under Contracts No. DE-AC02-06CH11357 and No. DE-FG02-91ER-40609, by the DFG under Grants No. Pi 393/2-2 and No. SFB 634, by the German-Bulgarian exchange program under Grants No. D/08/02055 and No. DO02-25, by the Bulgarian NSF under Contract No. DO 02-219, and by the Helmholtz International Center for FAIR.

[1] A. Arima and F. Iachello, Phys. Rev. Lett. **35**, 1069 (1975).
[2] F. Iachello and A. Arima, *The Interacting Boson Model* (Cambridge University Press, Cambridge, 1987).
[3] A. Arima and F. Iachello, Ann. Phys. (NY) **99**, 253 (1976).
[4] A. Arima and F. Iachello, Ann. Phys. (NY) **111**, 201 (1976).
[5] A. Arima and F. Iachello, Phys. Rev. Lett. **40**, 385 (1978).
[6] A. Bohr, Mat. Fys. Medd. K. Dan. Vidensk Selsk. **26**, 14 (1952).
[7] L. Wilets and M. Jean, Phys. Rev. **102**, 786 (1956).
[8] J. A. Cizewski *et al.*, Phys. Rev. Lett. **40**, 168 (1978).
[9] H. G. Borner, J. Jolie, S. Robinson, R. F. Casten, and J. A. Cizewski, Phys. Rev. C **42**, R2271 (1990).
[10] R. F. Casten and P. von Brentano, Phys. Lett. B **152**, 22 (1985).
[11] U. Neuneyer *et al.*, Nucl. Phys. A **607**, 299 (1996).
[12] A. Gade *et al.*, Nucl. Phys. A **665**, 268 (2000).
[13] V. Werner, H. Meise, I. Wiedenhover, A. Gade, and P. von Brentano, Nucl. Phys. A **692**, 451 (2001).
[14] G. Rainovski *et al.*, Phys. Lett. B **683**, 11 (2010).
[15] L. Coquard *et al.*, Phys. Rev. C **80**, 061304(R) (2009).

[16] G. Rainovski *et al.*, Phys. Rev. Lett. **96**, 122501 (2006).
[17] D. Pelte and D. Schwalm, in *Heavy Ion Collisions*, edited by R. Bock, Vol. 3 (North-Holland, Amsterdam, 1982), p. 1.
[18] I. Lee, Nucl. Phys. A **520**, 641 (1990).
[19] P. Nolan, F. Beck, and D. Fossan, Annu. Rev. Nucl. Part. Sci. **45**, 561 (1994).
[20] W. Liebherz *et al.*, Phys. Lett. B **240**, 38 (1990).
[21] F. Seiffert *et al.*, Nucl. Phys. A **554**, 287 (1993).
[22] P. F. Mantica Jr., B. E. Zimmerman, W. B. Walters, J. Rikovska, and N. J. Stone, Phys. Rev. C **45**, 1586 (1992).
[23] J. Katakura and K. Kitao, Nucl. Data Sheets **97**, 765 (2002).
[24] K. Alder *et al.*, Rev. Mod. Phys., 28 (1956).
[25] S. Raman, C. W. Nestor, and P. Tikkanen, At. Data Nucl. Data Tables **78** (2001).
[26] W. F. Mueller *et al.*, Phys. Rev. C **73**, 014316 (2006).
[27] F. Iachello, Phys. Rev. Lett. **53**, 1427 (1984).
[28] L. Coquard, Ph.D. thesis, Technische Universität Darmstadt, 2010.
[29] O. Scholten, Computer codes PHINT and FBEM, KVI Report No. 63 (1979).
[30] D. Bonatsos, D. Lenis, N. Pietralla, and P. A. Terziev, Phys. Rev. C **74**, 044306 (2006).